The Development of M^{3+}-Doped Mesoporous Ti_4O_7 Electrode for Pharmaceutical Degradation in Fresh Human Urine

Hsuan-Yu Kao

A thesis

submitted in partial fulfillment of the

requirements for the degree of

Master of Science

University of Washington

2022

Committee:

Hugh Hillhouse

David Beck

Program Authorized to Offer Degree:

Chemical Engineering

University of Washington

Abstract

The Development of M^{3+}-Doped Mesoporous Ti_4O_7 Electrode for Pharmaceutical Degradation in Fresh Human Urine

Hsuan-Yu Kao

Chair of the Supervisory Committee:

Hugh Hillhouse

Department of Chemical Engineering

An ideal electrode material for pharmaceutical degradation should be efficient, low-cost, and stable. However, none of the well-studied anode material has a lifetime of more than 400 hours. In this work, we fabricate metal with valence number three (M^{3+}) doped-mesoporous Ti_4O_7 planner electrodes. The electrode stability and pharmaceutical degradation performance are collected by galvanostatic test and pharmaceutical degradation rate in a full synthetic urine matrix with four common pharmaceuticals. Our results show that the Cobalt (Co^{3+}) doped-mesoporous Ti_4O_7 electrodes have a 30 hours lifetime and were able to degrade 96.7% sulfamethoxazole (SMX) within 60 minutes. In conclusion, the Co-doped mesoporous Ti_4O_7 electrodes have better stability than previous well-studied electrode materials and cheaper fabrication cost than boron-doped diamond electrodes. The electrode lifetime of the Co-doped mesoporous Ti_4O_7 electrode still can be further improved by increasing Co loading.

1. Introduction

Electrochemical advanced oxidation is a prospering method for wastewater treatment with its high pollutants degradation rate and no second pollutant generated [1]. To enhance the electrooxidation reaction, highly catalytic, highly stable, and low-costed electrodes are needed [2]. In recent electrode development studies, boron-doped diamond (BDD), lead oxide (PbO_2), and iridium oxide (IrO_2) electrodes. BDD is a well-studied material for electrooxidation reaction and allows generating *in-situ* hydroxyl radical (·OH) with a high reaction rate (k_{obs} = 10^9 $M^{-1}S^{-1}$) and stability (150 hr) [2-3]. However, BDD electrodes have a high fabrication cost, which hinders BDD electrodes from industrializing, since BDD electrodes are made by using the chemical vapor deposition (CVD) on titanium substrates [3-4]. To lower the cost without decreasing electrooxidation performance, IrO2 electrodes and PbO_2 electrodes are studied with their high stability. Nevertheless, IrO_2 electrodes have relatively low oxygen evolution potential (OEP) (1.7 V) compared to BDD electrode (3.3 V) due to chemisorb effect of OH radical and IrO_2 surface, and then form Ir-O-H complex [5-6]. The chemisorb of ·OH radical on the IrO_2 surface hinders ·OH radical from reacting with contaminants compounds in bulk solution. Meanwhile, PbO_2 electrodes do have high OEP and high stability providing great electrooxidation performance but will release toxic lead ions (Pb^{2+}) during the degradation process [2]. Other dimensionless stable anodes (DSA) electrodes with noticeably improved electrochemical performance, including high contaminants degradation rate, OEP, and conductivity, are studied but are still suffered from short electrodes lifetime and low chemical stability [1-2]. Therefore, developing an ideal electrode for wastewater treatment with high catalysis properties, stability, and low fabrication cost is necessary to approach the electrochemical advanced oxidation method for wastewater treatment.

Among multiple candidate materials for electrocatalysts, Magnéli phases titanium oxide (Ti_xO_{2x-1}, where $4 \leqq x \leqq 10$) is known for the highly reduced phase of titanium suboxide with a lower bandgap than titanium dioxide (TiO_2) [7-9]. Ti_xO_{2x-1} has a promising catalytic performance of direct and indirect OH generation and high electroconductivity, especially Ti_4O_7 (where x=4), which has the greatest conductivity within all other Magnéli phases titanium oxide [7]. Magnéli phases titanium oxide can be fabricated by anodization and hydrogen atmosphere reduction. Noticeably, Ti_4O_7 fabricated by hydrogen atmosphere reduction method composed a longer lifetime (4 hr) than Ti_4O_7 fabricated by anodization (2 hr) [10]. The hydrogen atmosphere reduction pathway is the following equation:

$$Ti + TiO_2 + H_2 \rightarrow Ti_4O_7 + H_2O \quad (1)$$

The lifetime of pristine Ti_4O_7 is obviously too short to industrialize. However, this poor stability can be improved by doping metal with valence number three (M^{3+}) to stabilize Ti^{3+} within Ti_4O_7 electrodes. In Yang et al.'s work, they introduced cobalt-doped black titanium oxide nanotube arrays (Co-Black TiO_2 NTA) for latrine wastewater treatment with an electrode lifetime of over 200 hours, which is 50 times greater than pristine Ti_4O_7 nanotube array [10].

Nonetheless, Co-Black TiO_2 NTA electrodes failed after 200 hours due to low oxygen-cobalt atom interaction and cobalt atom leaching [10]. Therefore, in this work, we study the relation between doped-metal-oxygen interaction and electrode stability and aim to investigate a stable Ti_4O_7 electrode for wastewater treatment.

2. Experimental

2.A. Electrode Preparation

Mesoporous TiO_2 electrodes were prepared by drop-casting 16.67 wt % 30 NRD titania paste/ethanol solution onto titanium substrates. All the titanium substrates are pretreated by soaking titanium substrates into deionized water, acetone, and isopropyl alcohol in the ultrasonic cleaner, merging with 1 M oxalic acid, and then heated for 90 minutes, with a stir rate of 600 radii per minute (rpm) to remove the oxidation layer on titanium substrate. The 30 NRD titania paste was purchased from the Greatcell Solar Materials Pty Ltd., Australia. The coated titanium substrates were annealed in the cube furnaces at 450 °C for 30 minutes to form mesoporous TiO_2 electrodes.

M^{3+} doped mesoporous TiO_2 electrodes were prepared by dip-coating mesoporous TiO_2 electrodes into 250 mM $(M^{3+})_2(NO_3)_2$/ethanol solution. The $(M^{3+})_2(NO_3)_3$ in this work were $La_2(NO_3)_3$, $Co(NO_3)_2$, and $Al_2(NO_3)_3$, and all of them are from the Sigma-Aldrich, Inc., United State. The coated titanium substrates with M^{3+} doping were annealed in the cube furnaces at 450 °C for 30 minutes to form mesoporous M^{3+} doped TiO_2 electrodes (M-TiO_2).

Following by annealing, mesoporous Ti_4O_7 and M^{3+} doped mesoporous Ti_4O_7 electrodes were prepared by reducing mesoporous TiO_2 electrodes in the 5 % hydrogen atmosphere at 700 °C in the tube furnace in the Research Training Testbed at the University of Washington, United State, with a heating rate of 10 °C/min and a cooling rate of 5 °C /min to obtain a blue layer of Ti_4O_7 on the titanium substrate. The average mass loading of Ti_4O_7 was calculated by equation (2).

$$M_{Ti_4O_7} = \frac{(M_{T'} - M_s) \times 1000}{A} \quad (2)$$

Where $M_{Ti_4O_7}$ is mass loading of Ti_4O_7 (mg/cm^2), $M_{T'}$ is electrode mass before doping (g), M_s is mass of titanium substrate (g), A is electrode surface area 8.56 cm^2.

The sample names of M-Ti_4O_7 with different doped metal with valence number three, the number of dip coating process for doping M^{3+}, and Ti_4O_7 mass-loading were listed in **Table 1**.

Table 1. M-Ti_4O_7 sample list with different mass-loading of M^{3+} and Ti_4O_7.

Sample Name	Doped M^{3+}	# of dip-coating	Volume of titania ink (ml)	Ti_4O_7 mass-loading (mg/cm^2)
TiO_2	N/A	0	N/A	N/A
Ti_4O_7(1ml)	N/A	0	1	21.0
Ti_4O_7(3ml)	N/A	0	3	24.5
Ti_4O_7	N/A	0	4	25.7
Ti_4O_7(6ml)	N/A	0	6	28.6
Ti_4O_7(8ml)	N/A	0	8	40.3
Ti_4O_7(10ml)	N/A	0	10	33.8
La-Ti_4O_7	Lanthanum (La)	3	4	25.7
Al-Ti_4O_7	Aluminum (Al)	3	4	25.7
Co-Ti_4O_7	Cobalt (Co)	3	4	25.7
Co(10x)-Ti_4O_7	Cobalt (Co)	10	4	25.7

2.B. Material Characterizations

X-ray diffraction (XRD) spectrums were collected from Bruker D8 Discover with IμS 2-D XRD System at Molecular Analysis Facility in the University of Washington, the United States, after reduced in 5 % hydrogen atmosphere and pharmaceutical degradation to obtain the composition of electrodes as-synthesized and the electrode degradation factors. FEI XL830 dual-beam SEM-FIB at Molecular Analysis Facility in University of Washington, United State, was applied to acquire the surface morphology of as-synthesized before and after being reduced in 5 % hydrogen atmosphere, and after pharmaceutical degradation.

2.C. Electrochemical Properties

All the electrochemical properties, including Cyclic Voltammetry (CV) diagrams, pharmaceutical degradation rate, and electrode stability tests of M^{3+} -Ti_4O_7 electrodes, were measured by the Princeton Applied Research Potentiostat/Galvanostat Model 263A. 30 mM $KClO_4$ solution was the electrolyte for CVs and electrode stability tests. In CV tests, the cycle of 0, 4, -2, 0 V was applied to investigate the OEP and the bandgap of M^{3+}- Ti_4O_7 electrodes before and after wastewater treatments. The pharmaceutical degradation rate of M^{3+}-Ti_4O_7 was measured in Galvanostatic mode with a current density of 10 mA/cm^2. The fresh human urine matrix (FUM) and the cylindrical cell setup were the same as in our previous work [6]. 10 ppm cyclophosphamide (CP), carbamazepine (CBZ), sulfamethoxazole (SMX), and ibuprofen (IBP) were added in FUM as our wastewater matrix. Four pharmaceutical concentrations of the wastewater matrix which were collected on 0, 15, 30, 60, and 90 minutes were measured by Bruker Esquire Ion Trap High-Performance Liquid Chromatography-Mass Spectrometer (HPLC-MS) in the Department of Chemistry at the University of Washington, United State.

Pseudo-first-order rate constant, k_{obs} of pharmaceutical degradation rate can be calculated in equation (3). The electrode stability was obtained by Galvanostatic mode with a current density of 10 mA/cm^2 in 30 mM $NaClO_4$ electrolyte until the electrode failed.

$$k_{obs} = -\frac{dln[(C_t - C_0)/C_0]}{dt} \quad (3)$$

Where C_t is the pharmaceutical concentration in t minutes, C_0 is the initial pharmaceutical concentration.

2.D. Reaction and Mass-Transfer Kinetic Properties

Pseudo-first-order rate constant, k_{obs} of pharmaceutical degradation rate can also be calculated in equation (4). To obtain the actual reaction rate, k', from equation (4), the mass transfer coefficients, k_c, of the M-Ti_4O_7 electrodes were needed since we have already known the k_{obs} from the equation (3). Here, we applied the limited current technique experiment to investigate the mass transfer coefficients k_c[11]. The limiting current in equation (5) was obtained by applying a steady state linear sweep voltammetry (LSV) from open circuit potential (OCP) 0.24 to -0.5 V with a scan rate 5 mV/s. All LSVs were conducted in in 500 mM K_2CO_3, 5 mM $K_3[Fe(CN)_6]$, and 5 mM $K_4[Fe(CN)_6]$ with the same electrochemical cell setting in all electrochemical properties measuring. After all, the k_c can be calculated by plugging in the steady state limited current as measured into equation (5), and then further obtain the actual pharmaceutical degradation rate, k', by equation (4)

$$k_{obs} = \frac{1}{\frac{1}{k'} + \frac{1}{k_c}} \quad (4)$$

$$k_c = \frac{I_{lim}}{nAFC_b} \quad (5)$$

Where k' is the actual pharmaceutical degradation coefficients (min^{-1}), k_c is the mass transfer coefficients (min^{-1}), I_{lim} is the steady state limited current (A), n is the number of electrons involving in the reaction, A is actual electrode surface area, and C_b is the bulk electrolyte concentration.

3. Results and Discussion

3.A. XRD Analysis

Figure 1 (a) was the TiO_2 electrode after annealing in 450 ^oC for 30 minutes. The strongest peak at $2\theta = 25.3^\circ$ indicated the (101) surface of anatase titanium oxide after annealed the titania paste, and peak at $2\theta = 34.9^\circ, 40.0^\circ,$ and 62.8° is the (100), (101), and (110) surface of hexagonal titanium, which is our substrate. Terpineol ($C_{10}H_{18}O$) in titania paste and ethyl alcohol had evaporated during 450 ^oC annealing since there was no other peak presented in XRD diagram. After reduced in 5 % H_2 in Ar atmosphere, as **Figure 1 (c)** shows, for Ti_4O_7 with mass loading 25.7 mg/cm^2, all anatase titanium oxide was reduced into Magnéli phases

titanium oxide, including Ti_nO_{2n-1}, which $4 \leq n \leq 7$. Ti_4O_7 is the dominated species within all Magnéli phases with the presented of the strongest (10-2) surface at $2\theta = 20.7^{\circ}$, (1-20) surface at $2\theta = 26.3^{\circ}$, and all other Ti_4O_7 reference peaks in **Figure 7**.

For M-Ti_4O_7 electrodes, besides Ti and Ti_4O_7 peaks, the doped metal (Co, La, and Al) had replaced some of the Ti atom in the titanium oxide lattices. For Co-Ti_4O_7 electrode, Co_2TiO_4 and Ti_4Co_2O peaks in **Figure 8** had presented in the XRD diagrams, **Figure 1(e)**. Similarly, peaks of $La_2Ti_2O_7$ and $LaTiO_3$, which references peaks are in **Figure 9**, also presented in the La-Ti_4O_7 XRD diagram **Figure 1 (g)**; peaks of $Al_2Ti_7O_{15}$, Al_2TiO_5, and Al_3Ti, which references peaks are in **Figure 10**, were observed in Al-Ti_4O_7 electrode XRD diagram **Figure 1 (i)**. The XRD results of the Co-Ti_4O_7, La-Ti_4O_7, and Al-Ti_4O_7 electrodes confirmed that our chosen metal with valence number three, Co, La, and Al, had been successfully doped into our Ti_4O_7 electrodes.

The intensity of Ti_4O_7 peaks in our M-Ti_4O_7 electrodes decreased after pharmaceutical degradation and stability test. It is clear that in **Figure 1 (k)**, the Ti_4O_7 peaks intensity, which was the dominated species before the electrooxidation reaction, was dramatically decreased. Instead, peaks of $Ti_{10}O_{19}$, the higher oxidized Magnéli phase titanium oxide, and the TiO_2 rutile peaks shew up. The results indicated that the electrodes failed might because of the oxidation of Magnéli phase titanium oxide, which causing the loss of conductivity. Besides, the doped metal component peaks, such as (123) and (126) surfaces of $La_2Ti_2O_7$ at $2\theta = 39.9^{\circ}$ and 41.2°, were no longer presented in the XRD diagram. This implied that the electrode failed not only because of the oxidation of Magnéli phases titanium oxide, but also the leaching of doped metal with valence number three.

3.B. Surface Morphology

Porous structure was found in TiO_2 coating layer after annealing with pore size $0.1\ um$, as **Figure 1(b)** shows. The porous structure of TiO_2 coating layer allowed hydrogen to penetrate to inner layer and increase the reduction portion of TiO_2. After reduced, the pore size of Ti_4O_7 grew to $0.5\ um$, which can be seen in **Figure 1 (d)**. Compared to the nanotube array structure from anodization approach with same mass loading, mesoporous structure created larger catalyst surface area. The larger surface area was highly favorable during the heterogeneous reaction with its more reaction active sites.

After doping different metal with valence number three, the surface morphology of Co-Ti_4O_7, La-Ti_4O_7, and Al-Ti_4O_7 were quite different with each other's. Co-Ti_4O_7, and Al-Ti_4O_7 have similar pour size (about $0.5\ um$) with pure Ti_4O_7 electrodes. Small protrusions with diameter $40\ nm$ in Co-Ti_4O_7 and $20\ nm$ in Al-Ti_4O_7 were investigated. We suggested those protrusions to be the doped Co and Al components, since the diameter ratio of Co and Al is 0.074:0.050, which met our SEM observations in **Figure 1 (f)** and **(j).** However, for La-Ti_4O_7, we can see that the pore size expanded to $1.5\ um$ and the mesoporous structure slightly collapsed in **Figure 1 (h)**. The damage of mesoporous structure might because of the atomic

diameter of La ($0.106\ nm$), which was about two times larger than the Ti atoms ($0.068\ nm$). The doping of La atom replaced some of the Ti atoms and knocked off the mesoporous structure by the large atomic volumes.

The Co-Ti_4O_7 electrodes mesoporous structure collapsed after the stability test (**Figure 1 (l) (m)**) and wastewater treatment (**Figure 1 (n)**). Notice that in **Figure 1 (m)**, we observed some small pits on the mesoporous structure, which were not presented on the electrode surfaces before the electrooxidation reaction. As we mentioned earlier, we suggested that protrusions on the electrode surfaces were the doped metal component. Therefore, we suggested that the pits on the failed Co-Ti_4O_7 electrodes might be the vacancies of leaching metal with valence number three. This speculation also agreed with our XRD results for the failed Co-Ti_4O_7 electrode in **Figure 1 (k)**. As a result, we also speculate that the failure of M-Ti_4O_7 might also because of the leaching metal with valence number three.

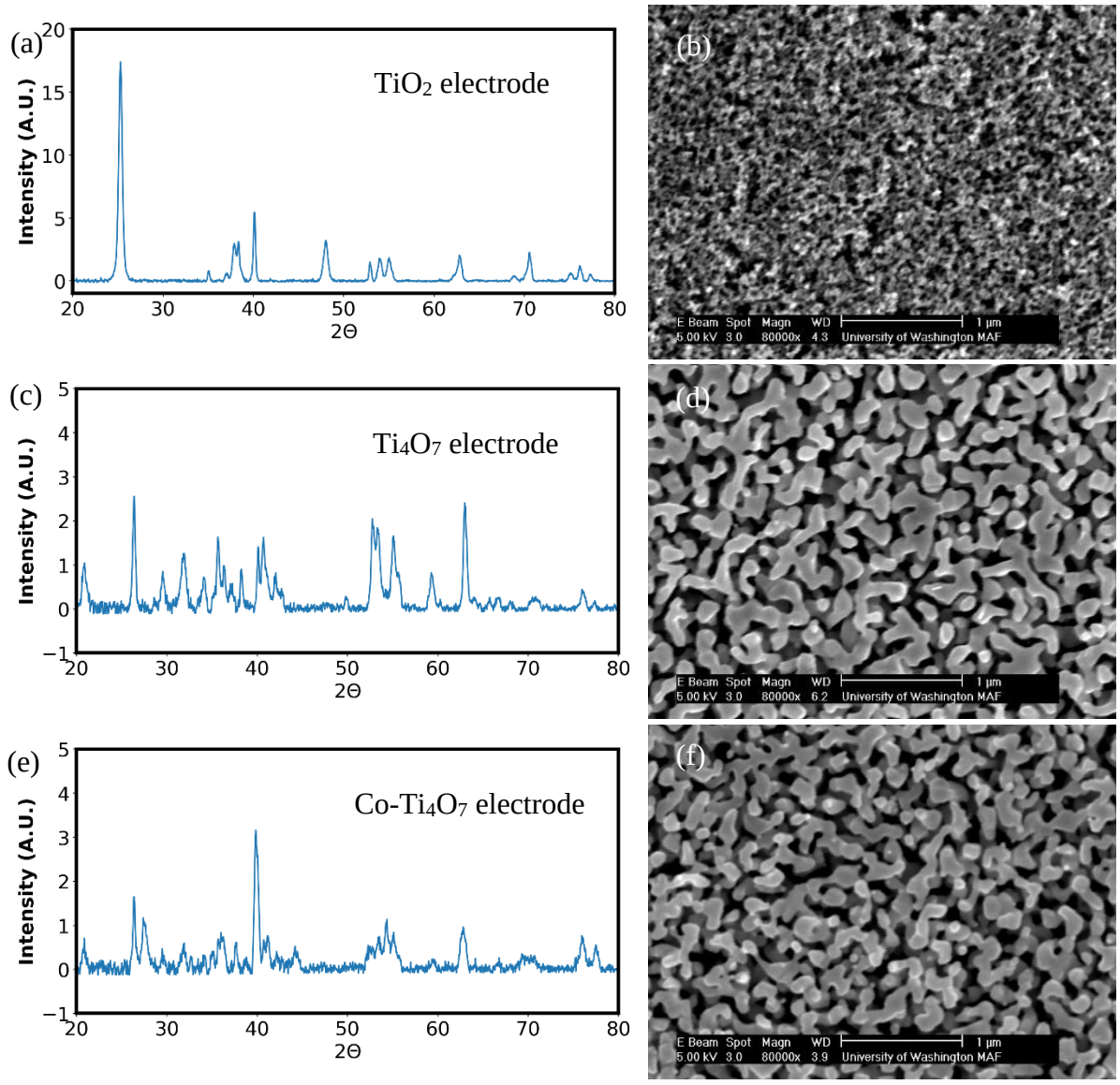

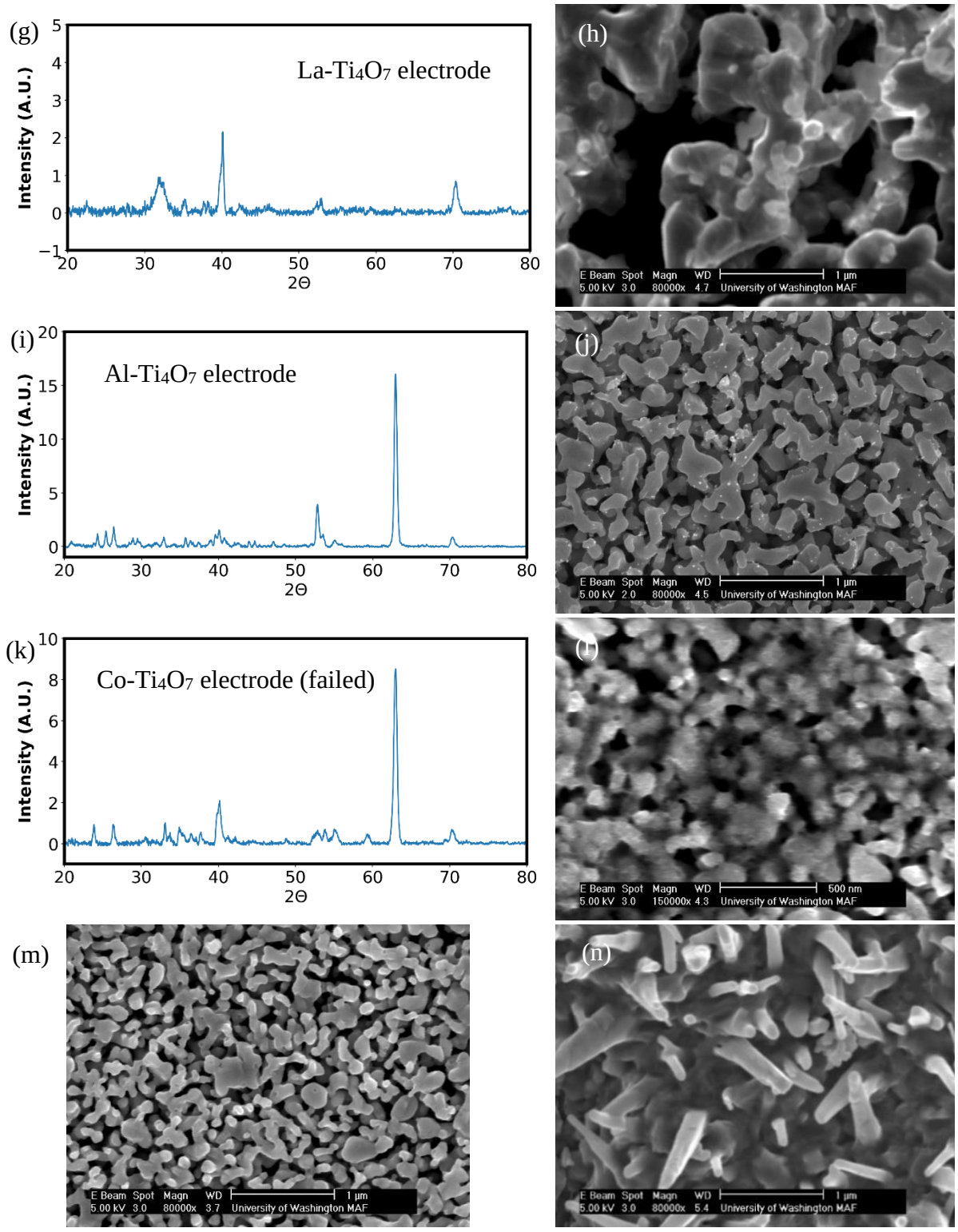

Figure 1. XRD diagrams and SEM images of (a)(b) TiO_2 electrode before reduced in the 5 % H_2 in Ar gas, (c)(d) Ti_4O_7 electrode, (e)(f) Co-Ti_4O_7 electrode, (g)(h) La-Ti_4O_7 electrode, and (i)(j) Al-Ti_4O_7 electrode after reduced in the 5 % H_2 in Ar gas, and (k)(l)(m)(n) Co-Ti_4O_7 electrode after pharmaceutical degradation.

3.C. Electrochemical properties

The cyclovoltammetry diagram of M-Ti_4O_7 electrodes, IrO_2 and BDD electrodes were in **Figure 2 (a)**. The OEP of pure Ti_4O_7 was 2.7 V, which was higher than the OEP of BDD

electrode (2.5 V), which allow more hydroxyl radical generated. High OEP is one of the advantages of pharmaceutical degradation with electrooxidation method since it allowed the hydroxyl radical formed first (at 2.5 V) without the oxygen evolution reaction competition (at 2.7 V). This made our undoped-Ti_4O_7 electrode become BDD-liked electrode instead of IrO_2-liked electrode. Meanwhile, our doped La-Ti_4O_7 and Al-Ti_4O_7 electrode also have the OEP 2.7 V, which were same as our undoped Ti_4O_7 electrodes. However, we noticed that the current response intensities of our Ti_4O_7, Co-Ti_4O_7, and La-Ti_4O_7 electrodes were quite different with each other while applying potential was larger than 2.7 V. The Al-Ti_4O_7 electrodes had larger current response (37 mA/cm^2) than Ti_4O_7 electrodes (18 mA/cm^2) while applied potential was 4 V, whereas the La-Ti_4O_7 electrodes had lower current response (12 mA/cm^2) than Ti_4O_7 electrodes (18 mA/cm^2). Current responses at the same applied voltage larger than 2.7 V here implied the oxygen evolution reaction rate. Therefore, we could conclude that the oxygen generation rate at our as synthesized electrodes was Al-Ti_4O_7 > Ti_4O_7 > La-Ti_4O_7. The reason of the different oxygen evolution rates was speculated to be the metal-oxygen bonding between the doped metal atoms and oxygen atoms. The different metal with valence number three with oxygen bonding energy was shown as **Table 2**. While the metal atom had a larger metal-oxygen bonding energy, which means they had stronger attraction between each metal and oxygen atoms, will hinder the oxygen generations. Notice that the OEP of Co-Ti_4O_7 electrodes (1.9 V) were much lower than the BDD electrodes. We suggested that was also due to the relative low Co-O interaction since the bonding energy of Co-O was only 384.5 kJ/mol. The low interaction between Co and oxygen atoms led to the easy escape of oxygen, which further led to the low OEP of Co-Ti_4O_7 electrodes, and hence made the Co-Ti_4O_7 electrode more IrO_2 liked.

Table 2. Bonding energy between oxygen and metal with valence number three (M^{3+}-O)

M^{3+}-O	Bonding Energy (kJ mol^{-1})	M^{3+}-O	Bonding Energy (kJ mol^{-1})
Co-O	384.5	Ti-O	672.4
Al-O	414.6	Sc-O	681.6
Ga-O	626.8	La-O	799.0

The galvanostatic diagram of Co-Ti_4O_7 electrodes, pure Ti_4O_7 electrodes with different mass-loading and BDD electrode during the pharmaceutical degradation in the full synthetic urine matrix is in **Figure 2 (b)**. All the galvanostatic experiments applied the same current density (10 mA/cm^2), therefore, the electrodes with lower potential at the potential-time diagram had the better conductivities. As the **Figure 2 (b)** shows, from mass loading below 25.7 mg/cm^2 (Ti_4O_7), the conductivity gradually increased as the mass loading increased. The conductivity improvement of Ti_4O_7 electrodes with higher Ti_4O_7 mass-loading might be due to the high conductivity of Ti_4O_7 itself, which is the most reduced Magnéli phases titanium oxide, and the titanium supporting substrate, further enhanced the conductivity of the composite Ti_4O_7 electrodes. Nevertheless, For the mass-loading greater than 25.7 mg/cm^2, the conductivities of Ti_4O_7 electrodes started to decrease, which may be due to the un-fully reduced layer of TiO_2

presented between the Ti substrate and the Ti_4O_7 coating layer since the coating layer getting much thicker while the mass-loading increased.

For the Ti_4O_7 electrode with mass loading 33 mg/cm^2, which marked as Ti_4O_7_1 ml in **Figure 2 (b)**, the electrode failed at the 30 minutes during the degradation. The reason for Ti_4O_7(1ml) electrode with mass loading 33 mg/cm^2 failed may be due to the low mass loading of Ti_4O_7 layer since we suggested the electrode failed due to the oxidation of Ti_4O_7 into TiO_2 and the coating layer peeling off. For the other Ti_4O_7 electrodes, which marked as Ti_4O_7(3ml), Ti_4O_7, Ti_4O_7(6ml), Ti_4O_7(8ml), and Ti_4O_7(10ml), the potential was stable during the 90 minutes pharmaceutical degradation process without many fluctuations. Thus, within the pure Ti_4O_7 electrodes with different Ti_4O_7 mass-loading, the one with 25.7 mg/cm^2 (Ti_4O_7) would be our optimized mass-loading Ti_4O_7 electrodes.

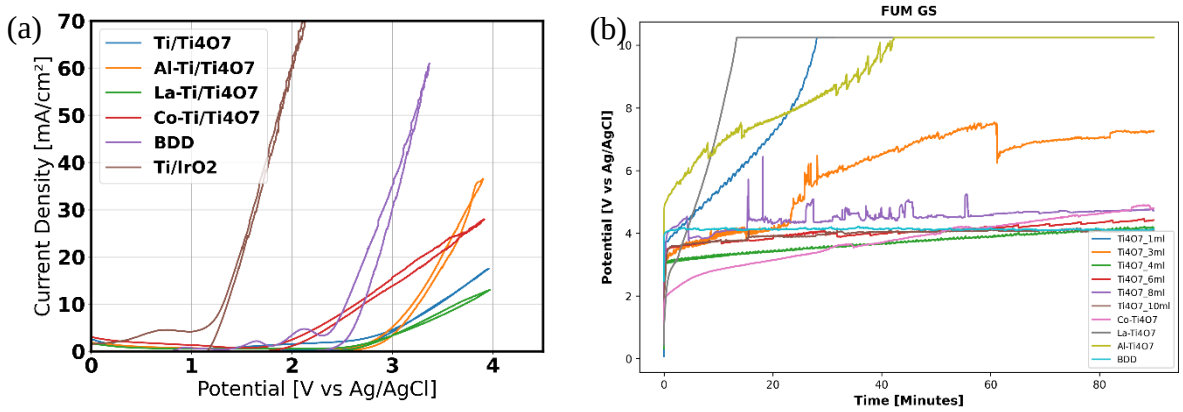

Figure 2. (a) Cyclovoltammetry diagram of M-Ti_4O_7 electrodes with different reduced time, IrO_2 and BDD electrodes. The OEP of Ti_4O_7, La-Ti_4O_7, and Al-Ti_4O_7 were greater than the BDD electrode, which might generate more ·OH radical than the electrode with lower OEP. (b) The galvanostatic diagram during the pharmaceutical degradations. For the pristine Ti_4O_7 electrode with different mass-loading, the Ti_4O_7(4ml) (mass-loading = 25.7mg/cm^2) had the best conductivity. With the same Ti_4O_7 mass-loading, the Co-Ti_4O_7 show the best conductivity among all M-Ti_4O_7 electrodes in FUM electrolyte.

Our Co-Ti_4O_7 and La-Ti_4O_7 electrode using our best Ti_4O_7 best mass-loading, surprisingly, failed quite fast in the FUM electrolyte. We suggested the reason might be that the composition of our FUM matrix was too complicated and might interact with our doped metal atoms. However, the true conductivity and stability of the M-Ti_4O_7 still needed to be examined in the next on stability tests using 30 mM $NaClO_4$ electrolyte.

3.D. Pharmaceutical degradation rate and pseudo-first order rate constant k_{obs}

The pharmaceutical degradation rate profiles for CP, CBZ, SMX, and IBF were shown in **Figure 3 (a)-(d)**. For the undoped Ti_4O_7 electrode, mass loading with 25.7 mg/cm^2 (which was Ti_4O_7) Ti_4O_7 coating showed the highest pharmaceutical degradation rate since SMX were almost fully decomposed at 60 minutes, and IBF were also fully decomposed after 90 minutes. Same optimal degradation rate also happed on CP and CBP in mass loading 25.7 mg/cm^2. We inferred that with mass loading lower than 25.7 mg/cm^2, the active area of our Ti_4O_7 electrodes

were also smaller. However, for mass loading higher than 25.7 mg/cm^2, the conductivity decreased due to uncomplete reduced TiO_2 or higher oxidation level Magnéli phase titanium oxide between Ti_4O_7 layer and Ti substrate since the reducing time were all 12 hours regardless any mass loading. With the same electrochemical cell geometry with our previous works [6], our mass transfer limiting rate using Ti_4O_7 was higher than using BDD electrode. We suggested that the higher mass transfer limiting rate was due to the mesoporous structure of our Ti_4O_7 electrode, whereas the BDD electrode was a planer structure. With the same surface area and mass loading, mesoporous structure provided more active surface area and thinner boundary layer which made the heterogeneous reaction taking place.

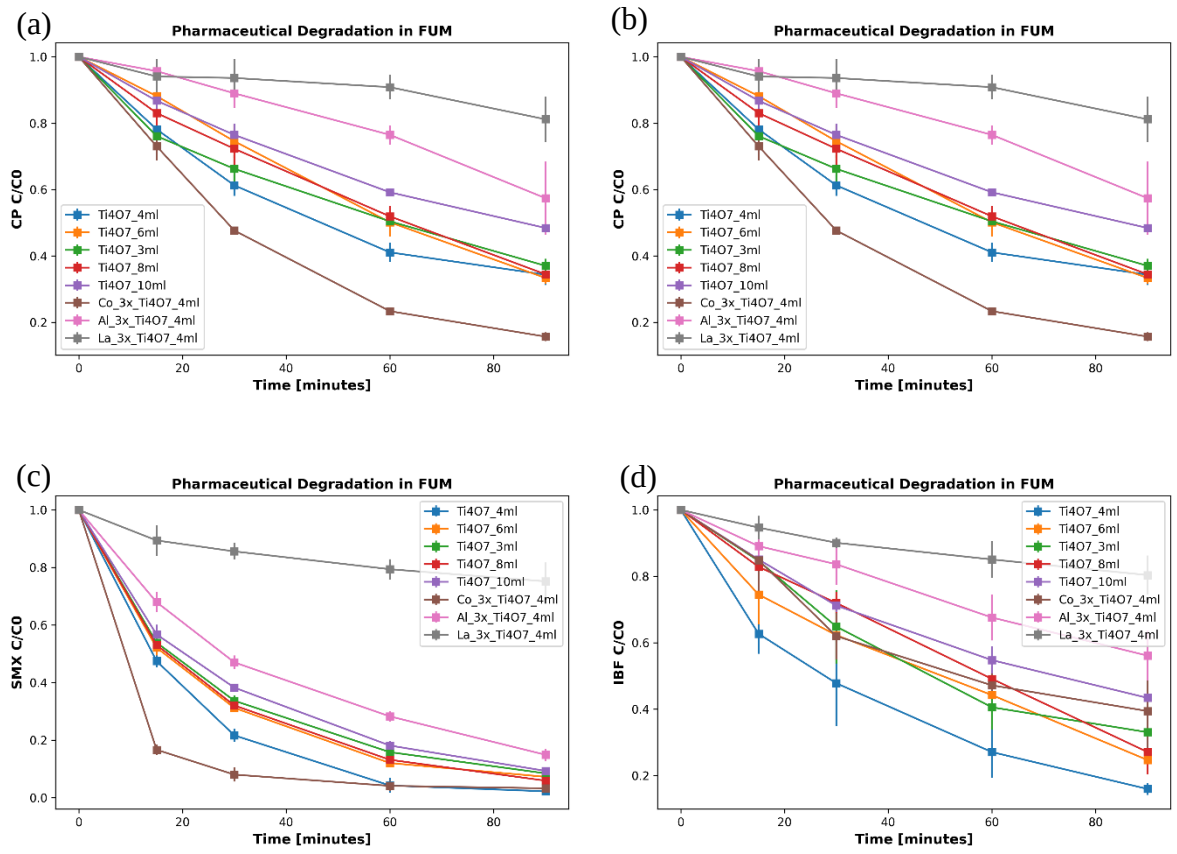

Figure 3. Pharmaceutical degradation profile of different M-Ti_4O_7 electrodes for (a) CP, (b)CBZ, (c) SMX, and (d) IBF. For the electrode with different Ti_4O_7 mass-loading, the Ti_4O_7(4ml) (mass-loading = 25.7mg/cm^2) had the best pharmaceutical degradation performance in four pharmaceuticals. With the best Ti_4O_7 mass-loading, the Co-doped one (Co-Ti_4O_7) had the best pharmaceutical degradation performance in CP, CBP, and SMX.

With the best Ti_4O_7 mass-loading, the Co-Ti_4O_7 electrodes pharmaceutical degradation performance was measured in the same experimental setting as before. We again investigated a huge improvement of CV, CBZ and SMX degradation in FUM matrix. SMX almost fully decomposed after the first 30 minutes, which was twice faster than the pure Ti_4O_7 electrodes. This dramatically increase of degradation rate, according to Yang et al.[10], was because of the increase oxygen vacancies in doped Co-Ti_4O_7 electrode, which caused by the weak Co-O interaction. The oxygen vacancies gave the Co-Ti_4O_7 electrodes more active sites for the

electrooxidation reactions. However, the the La-Ti_4O_7 and Al-Ti_4O_7 electrodes did not show any improvement in the four pharmaceutical degradation performance since the electrode already failed during the 90 minutes degradation treatment.

Table 3 was the pseudo-first-order-rate-constant, k_{obs}, of the four pharmaceutical degradation in FUM electrolyte using the equation (3), and the bar chart of k_{obs} was in **Figure 4**. Again, we observed that within all the different mass-loading of undoped Ti_4O_7 electrodes, the mass-loading 25.7 mg/cm^2 one had the largest k_{obs} in all four pharmaceuticals, and the Co-Ti_4O_7 with same Ti_4O_7 mass-loading (25.7 mg/cm^2) further increase the k_{obs}.

Table 3. The pseudo first order rate constant of four pharmaceutical with different Ti_4O_7 mass loading during pharmaceutical degradation in the full synthetic urine matrix.

	Observed Pseudo First Order Rate Constant, k_{obs} (min^{-1})			
Mass loading (ml)	CP	CBZ	SMX	IBP
1	0.0019	0.0062	0.0136	0.0075
3	0.0105	0.0195	0.0268	0.0129
4	0.0120	0.0206	0.0439	0.0198
6	0.0124	0.0217	0.0291	0.0148
8	0.0081	0.0092	0.0258	0.0119
10	0.0116	0.0157	0.0306	0.0142
4 (Co-doped)	0.0212	0.0270	0.0597	0.0105
4 (La-doped)	0.0020	0.0015	0.0029	0.0024
4 (Al-doped)	0.0061	0.0102	0.0206	0.0064

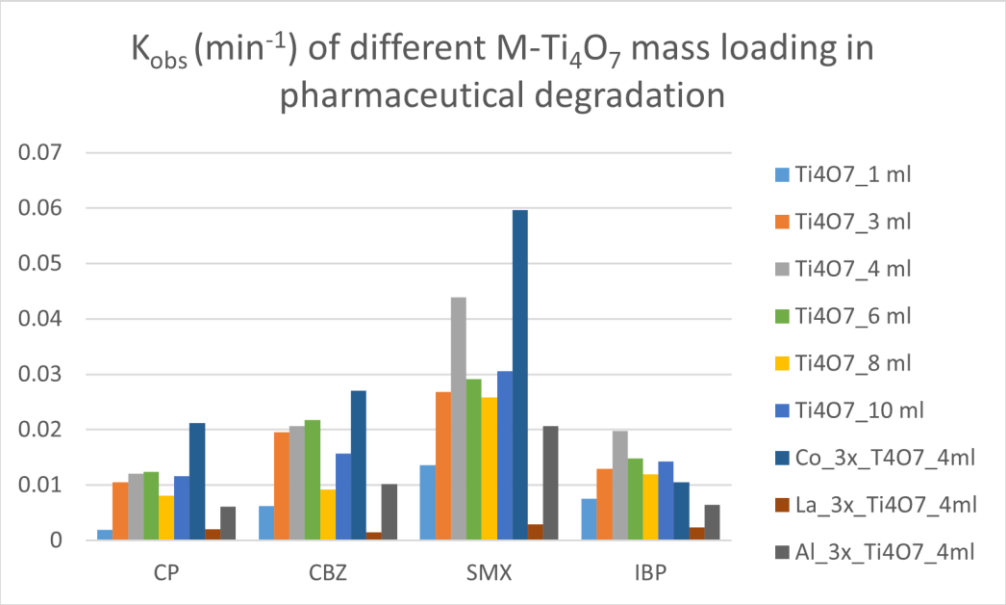

Figure 4. The observed-pseudo-first-order rate constant for four pharmaceutical degradations of different M-Ti_4O_7 electrodes. For the electrode with different Ti_4O_7 mass-loading, the Ti_4O_7(4ml) (mass-loading = 25.7mg/cm^2) had the best pharmaceutical degradation performance in four pharmaceuticals. With the best Ti_4O_7 mass-loading, the Co-doped one (Co-Ti_4O_7) had the best pharmaceutical degradation performance in CP, CBP, and SMX.

3.E. Electrode Stability Test

The sample compositions of our M-Ti_4O_7 electrodes in stability tests were listed in **Table 1**. For the undoped Ti_4O_7 electrodes, the electrode stability was 11.6 hours. This was 3 times more than the pure Ti_4O_7 electrodes (Black NTA electrodes) in Yang's work, which was 4.2 hours[10]. The large improved of our Ti_4O_7 electrodes were because of our heavy mass-loading, 25.7 mg/cm^2, whereas the Black NTA electrodes mass-loading in Yang et al. were only 6 mg/cm^2. Larger mass-loading could prevent the Ti_4O_7 from fully oxidized quickly. However, we could see in **Figure 5** that our Ti_4O_7 electrode was gradually lost its conductivity during the galvanostatic treatment with applied current 0.0856 A, which meant our Ti_4O_7 layer was not stabilized. To stabilize the Ti_4O_7 layer, the cobalt atoms were first chosen as our dopants to fabricate the Co-Ti_4O_7. The stability of Co-Ti_4O_7 electrodes was dramatically improved to 22.7 hours (49 % improvement) with just 3 times of dip-coating in 250 mM $Co(NO_3)_2$/EtOH solution. In **Figure 5**, the potential of Co-Ti_4O_7 electrode with 3 times of dip-coating process was remain in 2.1 V stably for 6.5 hours. The potential of Co-Ti_4O_7 started to increase after 6.5 hours with the similar trend with our undoped Ti_4O_7 electrode, which implying that the Co atoms might all leach out the Co-Ti_4O_7 electrode. As a result, we suggested the Co^{3+} was able to stabilize the Ti_4O_7. Larger Co mass-loading Co(10x)-Ti_4O_7 with 10 times of dip-coating process were fabricated, which denoted as Co_10x_ Ti_4O_7_4ml in **Figure 5**. The electrode lifetime again increased from 22.7 hours to 30.0 hours, which was another 24.3 % improvement. Notice that the potential remained 2.3 V stably for 12.7 hours and then started to increase with the similar trend of our undoped Ti_4O_7 electrodes, which was also speculated to be the fully leached of Co atoms. Thus, we concluded that Co atoms do help stabilizing the Ti_4O_7 electrodes but will still leaching during the electrooxidation reaction and leading to the failure of our electrodes. The further increase the electrode lifetimes of Co-Ti_4O_7 electrode still can be done by increasing the Co atoms loading. Here, we suggested that the sol-gel dip-coating solution can be applied instead of $Co(NO_3)_2$/EtOH solutions. The high viscosity of sol-gel method could help largely increase the Co loading within fewer times of dip-coating process.

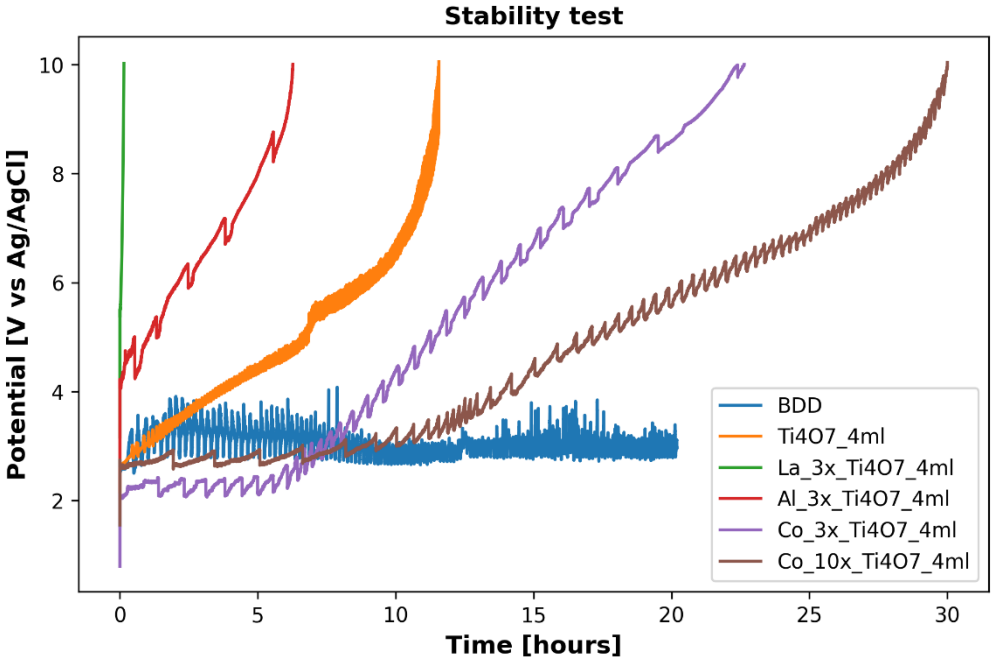

Figure 5. Stability test to M-Ti_4O_7 electrodes. Our pristine Ti_4O_7 electrode had a 11.6 hours lifetime, which is 3 times more than the Black NTA electrode in Yang et al.'s work. After doping M^{3+}, only the Co-Ti_4O_7 electrode had a significant improvement on the electrode lifetime. The decreased lifetime of Co-Ti_4O_7 and Co-Ti_4O_7 electrode was likely because the large radius difference between La and Ti atoms, and the radius difference between Al and Ti atoms. Also, by repeating Co dip-coating 10 times instead of 3 times, the electrode stability also increased from 22 hours to 30 hours.

The metal with valence number three (M^{3+}) doped sample, La-Ti_4O_7 and Al-Ti_4O_7 electrodes were made to see whether the stronger M-O bonding could prevent the doped metal leaching during the oxidation process. Surprisingly, the La-Ti_4O_7, which had the strongest M-O bonding energy, had the lowest electrode stability (0.14 hour), and then follow by Al-Ti_4O_7 (6.27 hours), which had the second large M-O bonding energy. The reasons of having opposite trend as we expected was speculated to be the large difference ionic radius between doped metal atoms (La, Al) and Ti atoms. The ionic radius of Ti, Co, La, and Al atoms were listed in **Table 4**. We noticed that the ionic radius between Ti and La, and between Ti and Al were much larger that the ionic radius between Ti and Co. Hence, the Al-Ti_4O_7 and La-Ti_4O_7 electrodes all failed faster than Co-Ti_4O_7 was likely because the crystal structure became less stable when Ti atoms were substitute by La and Al atoms.

Table 4. Ionic radius of Ti and doped M metals.

Elements	Ionic radius (nm)	Elements	Ionic radius (nm)
Ti	0.068	La	0.106
Co	0.074	Al	0.050

3.F. Reaction and Mass-Transfer Kinetic

According to the SEM image in **Figure 1**, our M-Ti_4O_7 electrodes, including Co-Ti_4O_7 and Al-Ti_4O_7 electrodes, had the mesoporous structure, which had a larger surface area than the flat BDD electrode that we used in our previous works[6]. With the larger surface area, we

speculated that our M-Ti_4O_7 electrodes would have a larger mass-transfer coefficient than the BDD electrodes since we all applied the same current, 0.0856 A to. The LSV of the Co-Ti_4O_7 electrode that conducted in the 500 mM K_2CO_3, 5 mM $K_3[Fe(CN)_6]$, and 5 mM $K_4[Fe(CN)_6]$ electrolyte was in **Figure 6**. We investigated that the limited current for the Ti_4O_7, Co-Ti_4O_7 and Al-Ti_4O_7 electrodes were 1.45, 1.23, and 1.70 mA/cm^2. By plugging in the limited current into equation (5), the mass-transfer rate constant for the Ti_4O_7, Co-Ti_4O_7 and Al-Ti_4O_7 electrodes, kc, were 0.040, 0.032, and 0.045 min^{-1}. However, since our electrochemical cell set up was the same, the mass-transfer rate of using BDD and our synthesized M-Ti_4O_7 electrode should be the same with the same stir rate, 600 rpm. By knowing the ratio between kc of BDD and kc of M-Ti_4O_7 electrodes, the actual electrode surface area of our M-Ti_4O_7 electrodes could be calculated. Therefore, we observed that the actual surface area of the Ti_4O_7, Co-Ti_4O_7, and Al-Ti_4O_7 electrodes were 12.23, 13.76, 9.78 cm^2.

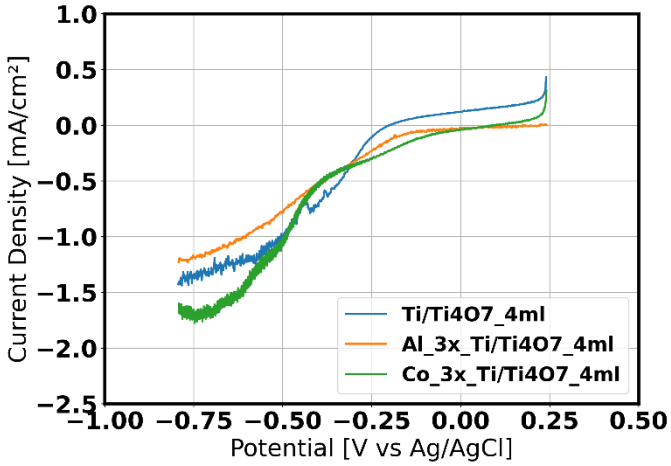

Figure 6. Mass transfer limiting rate of M-Ti_4O_7 electrodes using limiting current technique in 500mM K_2CO_3 electrolyte. The limiting current was different between Ti_4O_7, Co-Ti_4O_7, and Al-Ti_4O_7 electrode was due to the difference of surface area. With the limiting current observed, we could further calculated the actual electrode surface area of our M-Ti_4O_7 electrodes.

With a given k_{obs} and kc, the real reaction rate, k', of four pharmaceutical degradation rates in FUM matrix using our Ti_4O_7 and Co-Ti_4O_7 as the working electrodes could be calculated by equation (4). The calculated Ti_4O_7, Co-Ti_4O_7, Al-Ti_4O_7, BDD, and IrO_2 planer electrodes k' were listed in **Table 5**. We noticed that our Ti_4O_7 electrodes and Co-Ti_4O_7 electrodes had strong selectivity toward SMX. The Ti_4O_7 electrodes had the SMX rate constant k' 7.66 cm/min, and the Co-Ti_4O_7 electrodes had the SMX rate constant k' 18.71 cm/min, which were at least 40 times and 60 times more than the other three pharmaceuticals with the same working electrodes. The reason of the high selectivity to SMX degradation was the present of sulfur atoms presented in SMX molecules, and the sulfur atoms might have strong interactions with metal with valence number three as well. The relative low degradation rates toward CP, CBZ, and IBF were because the electrode active sites were mostly occupied by the SMX molecules. That the pharmaceutical degradation rate of Co-Ti_4O_7 electrodes were greater than the undoped

Ti_4O_7 electrodes was agree with Yang et al.'s works, which was suggested to be the increase of oxygen vacancies due to the weak Co-O bonding.

Table 5. Real reaction rate constant, k', of M-Ti_4O_7 electrodes for CP, CBZ, SMX, and IBF degradation rate in FUM matrix (normalized).

Working Electrode	CP k' (cm/min)	CBZ k' (cm/min)	SMX k' (cm/min)	IBF k' (cm/min)
Ti_4O_7	0.08	0.19	7.66	0.18
Co-Ti_4O_7	0.18	0.31	18.71	0.07
Al-Ti_4O_7	0.04	0.07	0.27	0.04
BDD	0.94	0.82	1.09	0.82
IrO_2	0.25	0.27	0.34	0.28

4. Conclusions

In this work, our results first show that our undoped mesoporous Ti_4O_7 electrodes did have a longer lifetime, 11.6 hours, than the black NTA electrode lifetime, 4.2 hours, in Yang et al.'s work due to a larger Ti_4O_7 mass-loading. Our M-Ti_4O_7 electrodes provided a greater mass transfer rate (0.040, 0.032, and 0.045 min^{-1}). However, the electrodes lifetime did not follow our expectation that the electrode lifetime would increase with the M-O bonding energy. In our results, stability degreased due to the large ionic radius difference between doped metal atoms and Ti atoms. Within different M^{3+}, the Co-Ti_4O_7 had the best electrode lifetime among La-Ti_4O_7 and Al-Ti_4O_7. Meanwhile, increasing Co loading also could further improved the electrode stability. The Co(10x)-Ti_4O_7 had the longest lifetime, 30.0 hours, within all our M-Ti_4O_7 electrodes. Noticeably, our Ti_4O_7 and Co-Ti_4O_7 electrodes had a high selectivity toward SMX than other three pharmaceuticals in FUM matrix. To further increase our Co-Ti_4O_7 electrode lifetime, we will apply sol-gel method for doping Co atoms instead of $Co(NO_3)_2$/EtOH for increasing the viscosity and thus fabricate a heavier Co-doped Ti_4O_7 electrode. This will be expecting to be significantly improves the electrode lifetime with our simple, eco-friendly material and fabrication method, which allows further application on wastewater treatment and promote the development of electrooxidation method utilized in wastewater treatment plants.

5. Appendix

5.A. XRD Reference Peaks

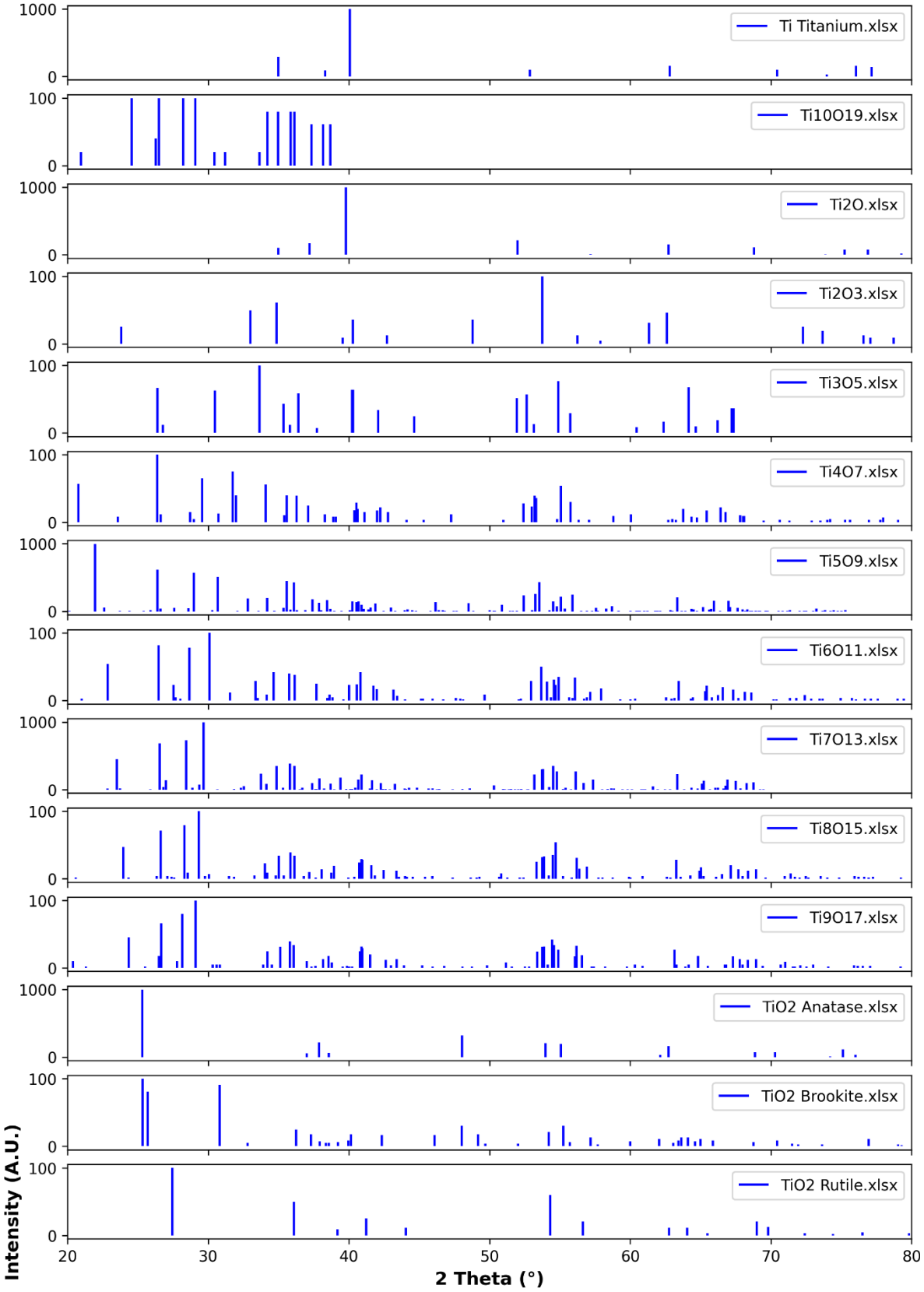

Figure 7. Reference peaks of pure titanium oxide and titanium suboxide compounds.

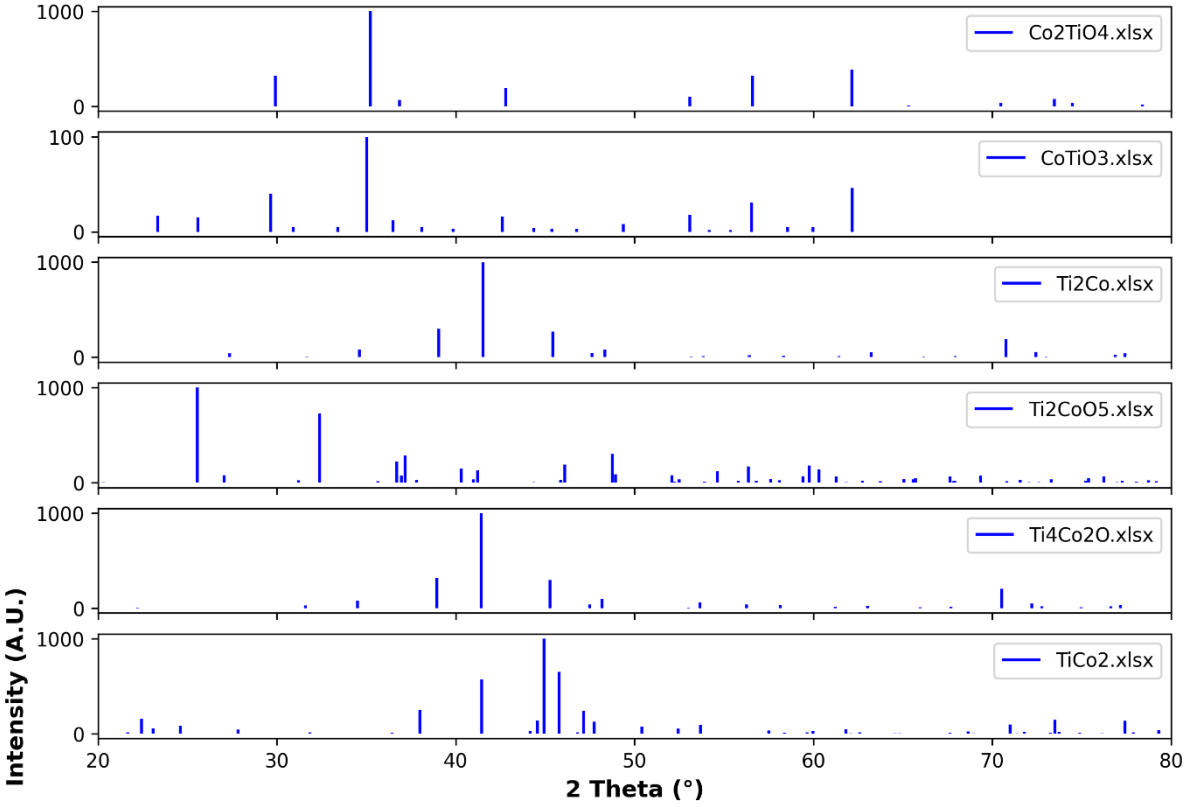

Figure 8. Reference peaks of cobalt doped titanium oxide and titanium suboxide compounds.

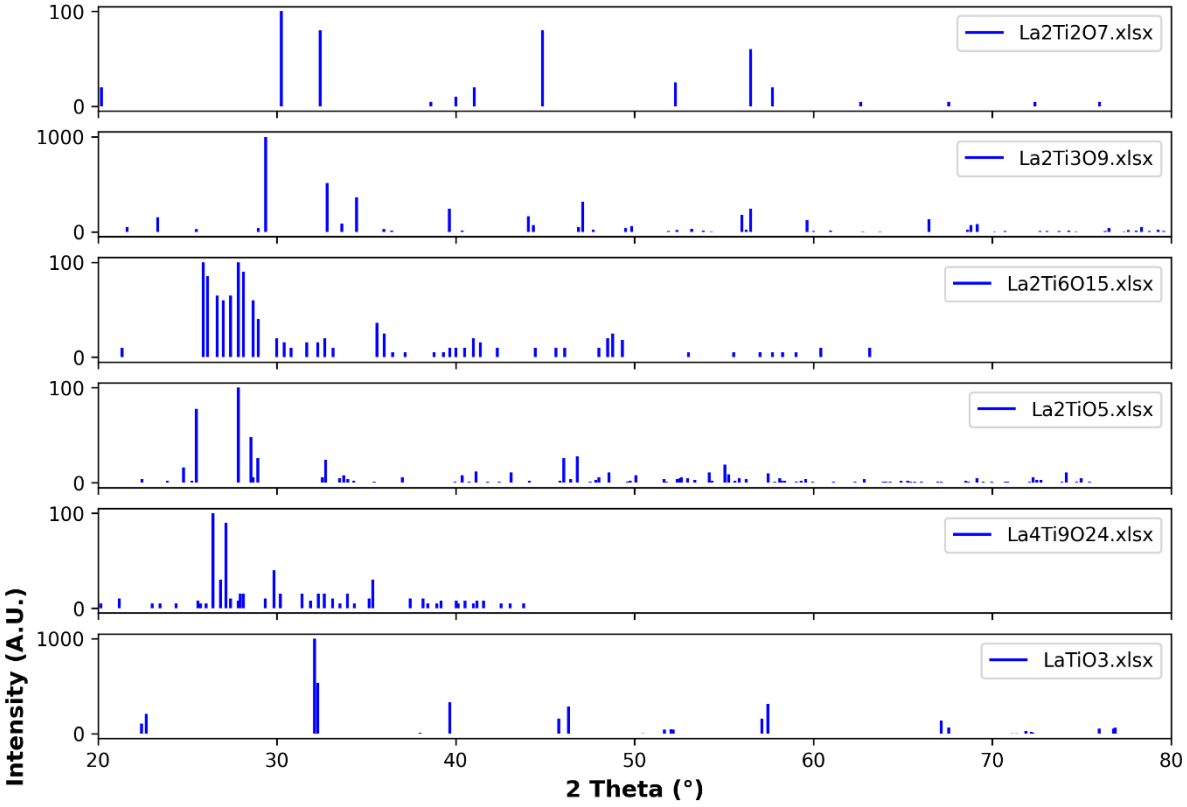

Figure 9. Reference peaks of lanthanum doped titanium oxide and titanium suboxide compounds.

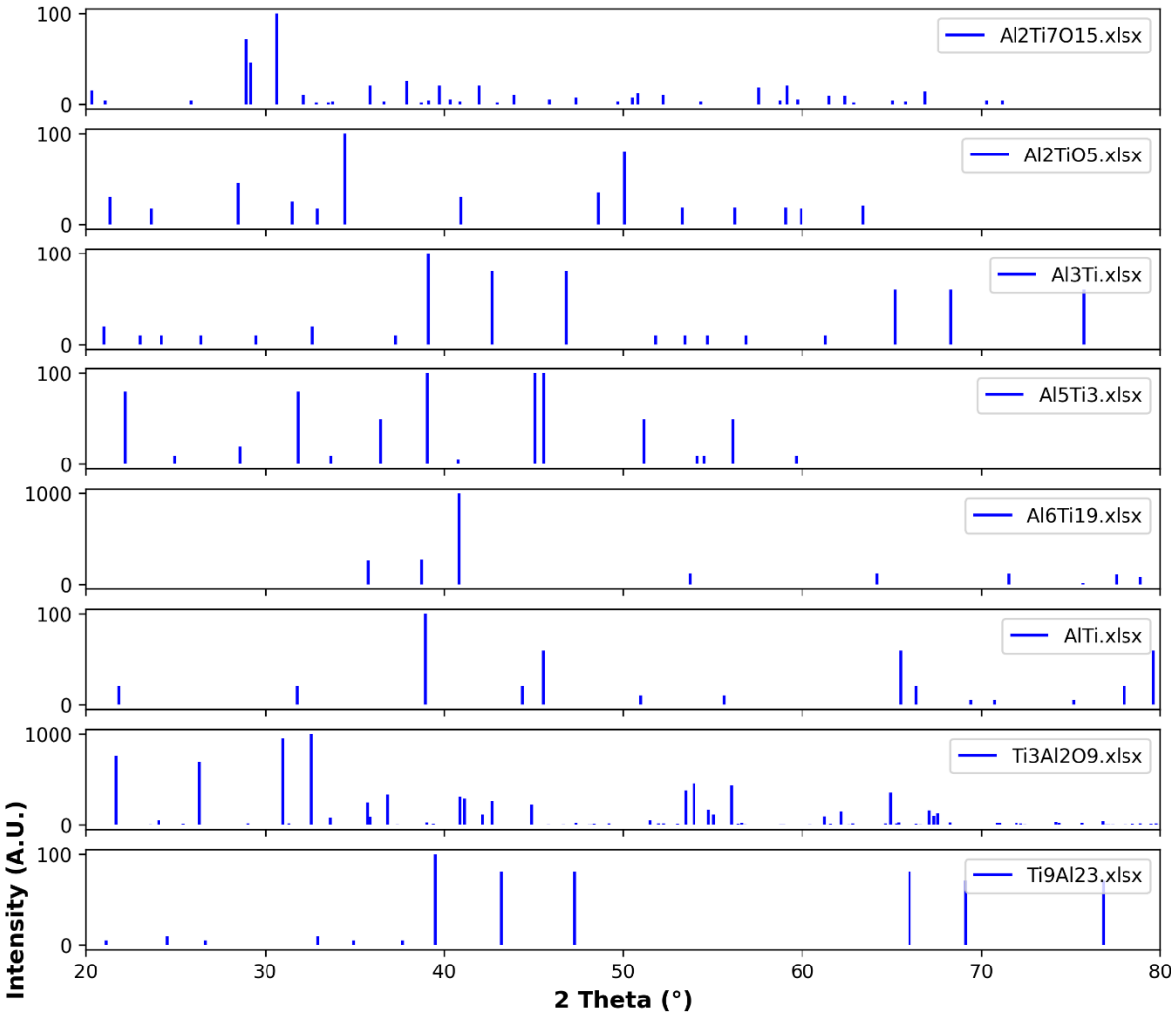

Figure 10. Reference peaks of aluminum doped titanium oxide and titanium suboxide compounds.

6. Reference

1. Särkkä, H.; Bhatnagar, A.; Sillanpää, M., Recent developments of electro-oxidation in water treatment—a review. *Journal of Electroanalytical Chemistry* **2015,** *754*, 46-56.
2. Wu, W.; Huang, Z.-H.; Lim, T.-T., Recent development of mixed metal oxide anodes for electrochemical oxidation of organic pollutants in water. *Applied Catalysis A: General* **2014,** *480*, 58-78.
3. Miao, D.; Liu, T.; Yu, Y.; Li, S.; Liu, G.; Chen, Y.; Wei, Q.; Zhou, K.; Yu, Z.; Ma, L., Study on degradation performance and stability of high temperature etching boron-doped diamond electrode. *Applied Surface Science* **2020,** *514*, 146091.
4. Yokoya, T.; Nakamura, T.; Matsushita, T.; Muro, T.; Takano, Y.; Nagao, M.; Takenouchi, T.; Kawarada, H.; Oguchi, T., Origin of the metallic properties of heavily boron-doped superconducting diamond. *Nature* **2005,** *438* (7068), 647-650.
5. Cherevko, S.; Reier, T.; Zeradjanin, A. R.; Pawolek, Z.; Strasser, P.; Mayrhofer, K. J., Stability of nanostructured iridium oxide electrocatalysts during oxygen evolution reaction in acidic environment. *Electrochemistry Communications* **2014,** *48*, 81-85.
6. Clark, J. A.; Yang, Y.; Ramos, N. C.; Hillhouse, H. W., Selective oxidation of pharmaceuticals and suppression of perchlorate formation during electrolysis of fresh human urine. *Water Research* **2021,** *198*, 117106.
7. Lee, W., Magnéli phase TiO2 and their thermoelectric properties. **2020**.
8. Smith, J.; Walsh, F.; Clarke, R., Electrodes based on Magnéli phase titanium oxides: the properties and applications of Ebonex® materials. *Journal of applied electrochemistry* **1998,** *28* (10), 1021-1033.
9. Yang, Y.; Hoffmann, M. R., Synthesis and stabilization of blue-black TiO2 nanotube arrays for electrochemical oxidant generation and wastewater treatment. *Environmental science & technology* **2016,** *50* (21), 11888-11894.
10. Yang, Y.; Kao, L. C.; Liu, Y.; Sun, K.; Yu, H.; Guo, J.; Liou, S. Y. H.; Hoffmann, M. R., Cobalt-doped black TiO2 nanotube array as a stable anode for oxygen evolution and electrochemical wastewater treatment. *ACS catalysis* **2018,** *8* (5), 4278-4287.
11. Selman, J. R.; Tobias, C. W., Mass-transfer measurements by the limiting-current technique. In *Advances in chemical engineering*, Elsevier: 1978; Vol. 10, pp 211-318.